

Cite this: *Chem. Sci.*, 2015, **6**, 70Received 25th August 2014  
Accepted 18th September 2014

DOI: 10.1039/c4sc02591a

[www.rsc.org/chemicalscience](http://www.rsc.org/chemicalscience)

## Carbon–hydrogen (C–H) bond activation at Pd<sup>IV</sup>: a Frontier in C–H functionalization catalysis

Joseph J. Topczewski and Melanie S. Sanford\*

The direct functionalization of carbon–hydrogen (C–H) bonds has emerged as a versatile strategy for the synthesis and derivatization of organic molecules. Among the methods for C–H bond activation, catalytic processes that utilize a Pd<sup>II</sup>/Pd<sup>IV</sup> redox cycle are increasingly common. The C–H activation step in most of these catalytic cycles is thought to occur at a Pd<sup>II</sup> centre. However, a number of recent reports have suggested the feasibility of C–H cleavage occurring at Pd<sup>IV</sup> complexes. Importantly, these latter processes often result in complementary reactivity and selectivity relative to analogous transformations at Pd<sup>II</sup>. This mini review highlights proposed examples of C–H activation at Pd<sup>IV</sup> centres. Applications of this transformation in catalysis as well as mechanistic details obtained from stoichiometric model studies are discussed. Furthermore, challenges and future perspectives for the field are reviewed.

### Introduction

Over the past 15 years, catalytic C–H bond functionalisation has emerged as a rich and highly active field of research.<sup>1</sup> C–H functionalisation reactions proceeding *via* Pd<sup>II/IV</sup> catalytic cycles are particularly prevalent due to their operational simplicity, wide scope, excellent functional group tolerance, and opportunities to access both C–C and C–heteroatom bond construction.<sup>2</sup> Pd<sup>II/IV</sup>-catalysed C–H functionalization reactions are generally proposed to proceed *via* catalytic cycles exemplified by that

shown in red in Fig. 1. This involves three elementary steps: C–H activation at Pd<sup>II</sup>, 2e<sup>–</sup> oxidation to Pd<sup>IV</sup> (or a Pd<sup>III</sup> dimer)<sup>3</sup> with an appropriate stoichiometric oxidant (oxidant-X), and finally C–X bond-forming reductive elimination from the high valent palladium centre to release the product.

Extensive research has established that the steps occur in this order for the vast majority of Pd<sup>II/IV</sup>-catalysed C–H functionalisations.<sup>2</sup> However, several recent reports have suggested that C–H cleavage can also occur at Pd<sup>IV</sup> centres (Fig. 1, blue) and, further, that this process may be governed by different selectivity and reactivity principles than analogous transformations at Pd<sup>II</sup>. This offers the exciting possibility for alternative catalytic cycles for Pd-catalysed C–H functionalisation,

Department of Chemistry, University of Michigan, Ann Arbor, MI, 48108, USA. E-mail: [mssanfor@umich.edu](mailto:mssanfor@umich.edu); Fax: +1 734 647 4865; Tel: +1 734 615 0451



Joseph Topczewski earned a B.S. with honours from the University of Wisconsin-Parkside in 2007 and conducted research with Professor Lori Allen. He received his Ph.D. in 2011 from the University of Iowa and was named an ACS Medicinal Chemistry Predoctoral Fellow while conducting research in the lab of David F. Wiemer. At the University of Iowa, he conducted postdoctoral studies with

Professors Hien Nguyen and Daniel Quinn before joining the Sanford Lab in 2013. He is currently an NIH NRSA postdoctoral fellow studying the application of high valent transition metal catalysis.



Melanie Sanford obtained her B.S. and M.S. degrees from Yale University and conducted research with Professor Robert Crabtree. She completed her Ph.D. at the California Institute of Technology with Professor Robert Grubbs and conducted postdoctoral research with Professor John Groves at Princeton University before joining the faculty at the University of Michigan in 2003. After receiving numerous awards, she was promoted in 2007 and 2010 and is currently the Moses Gomberg Collegiate Professor of Chemistry. The Sanford lab is engaged in unveiling the reactivity of high valent transition metals and elucidating the mechanism of this reactivity.



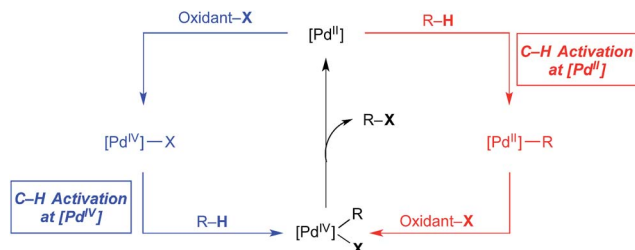


Fig. 1 Examples of catalytic cycles involving C–H activation at Pd<sup>II</sup> (red) versus Pd<sup>IV</sup> (blue).

involving, for example, oxidation of Pd<sup>II</sup> to Pd<sup>IV</sup>, C–H bond activation at Pd<sup>IV</sup>, and reductive elimination to release the product and regenerate the Pd<sup>II</sup> catalyst. Notably, in both cycles in Fig. 1, additional and/or alternative steps are possible; however, the key distinguishing feature of the blue cycle, discussed herein, is that at least one C–H activation event occurs at Pd<sup>IV</sup>. This mini review summarizes examples where arene C–H activation at a Pd<sup>IV</sup> centre is proposed in both catalytic transformations and in stoichiometric model systems.<sup>4</sup> For some of these systems, clear experimental evidence demonstrates C–H activation at Pd<sup>IV</sup> while for others, the role of C–H activation at Pd<sup>IV</sup> is strongly suspected. Both synthetically useful catalytic cycles and mechanistic details are presented and discussed.<sup>5</sup>

## C–H activation at Pd<sup>IV</sup>

To the best of our knowledge, the first report implicating a C–H activation reaction at Pd<sup>IV</sup> involved the dimerization of 2-aryl pyridines.<sup>6</sup> In this system, Pd(OAc)<sub>2</sub> catalyses the C–H/C–H oxidative coupling of a variety of substituted 2-aryl pyridines at room temperature using Oxone as the terminal oxidant. A representative example is the conversion of 2 equiv. of **1** into **2** (Fig. 2).

Several experiments were conducted that suggest that this transformation involves two discrete C–H activation steps that have very different selectivities. For example, the unsymmetrically-substituted substrate **3** undergoes stoichiometric cyclo-metallation with Pd<sup>II</sup>(OAc)<sub>2</sub> to afford a single isomeric product **4** via selective cleavage of C–H<sub>A</sub> (Fig. 3a). When this complex is subjected to Oxone and substrate **1** under the standard conditions, a single isomer of the coupled product is formed (**6a**, Fig. 3c). In contrast, when the sequence is reversed (*i.e.*, **1** is first cyclometallated at Pd<sup>II</sup> to form **5** (Fig. 3b), and this intermediate is subjected to analogous conditions with substrate **3**), a 5 : 1

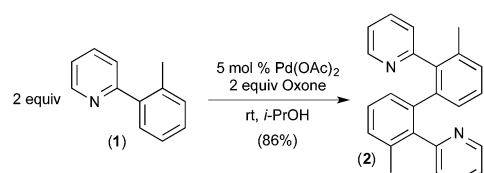


Fig. 2 Oxidative coupling of 2-arylpyridine derivatives via proposed C–H activation at Pd<sup>IV</sup>.

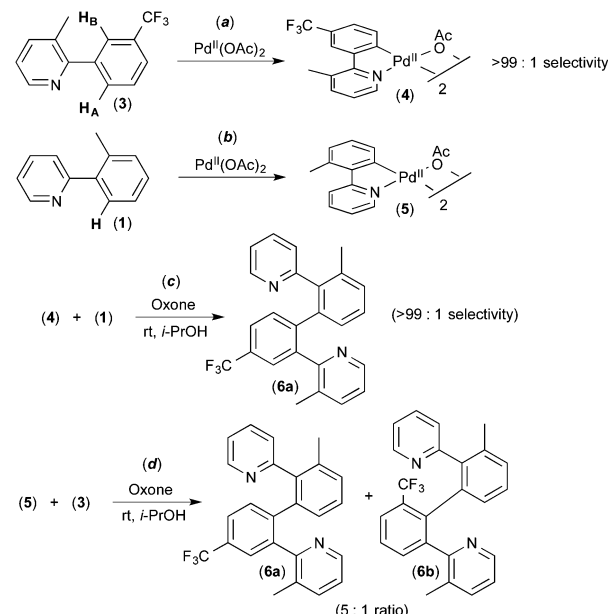


Fig. 3 Experiments implicating two different C–H activation steps with different selectivities in activation of substrate **3**.

mixture of the isomeric products **6a** and **6b** is produced (Fig. 3d). These results implicate two different C–H activation steps with different selectivities: (i) the initial cyclometalation of **3** at Pd<sup>II</sup>(OAc)<sub>2</sub> (>99 : 1 selectivity for activation of H<sub>A</sub>) and (ii) a subsequent C–H activation of **3** (5 : 1 selectivity for H<sub>A</sub> *versus* H<sub>B</sub>).

A variety of additional experiments, including cross-over studies and reactivity studies of possible intermediates, implicated the mechanism shown in Fig. 4. Here, an initial C–H activation at Pd<sup>II</sup> (step (i)), is followed by oxidation of the resulting palladacycle intermediate A with Oxone to yield Pd<sup>IV</sup> species B (step (ii)). The second C–H activation then occurs at this Pd<sup>IV</sup> intermediate to yield C (step (iii)), which undergoes C–C bond-forming reductive elimination to complete the catalytic cycle (step (iv)).

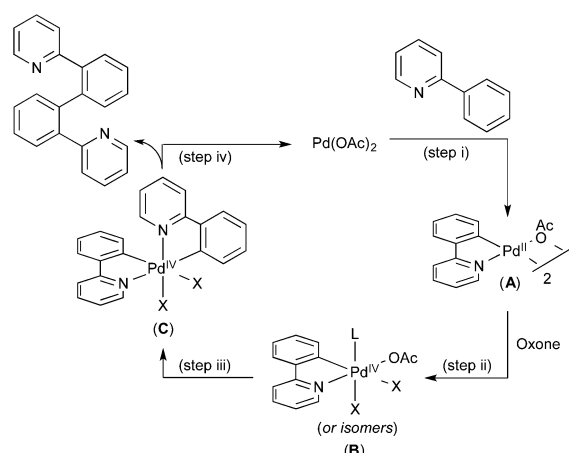


Fig. 4 Proposed mechanism for Pd-catalysed oxidative coupling of 2-aryl pyridines.



## Synthetic applications of C–H activation at Pd<sup>IV</sup>

Subsequent work has taken advantage of proposed arene C–H activation reactions at Pd<sup>IV</sup> to achieve synthetically useful catalytic transformations. In one elegant example, Michael demonstrated the Pd<sup>II/IV</sup>-catalysed aminoarylation of terminal olefins with NFSI as the oxidant (Fig. 5).<sup>7</sup> This reaction was discovered during an investigation of the Pd-catalysed diamination of 7 (Fig. 5a). When the solvent for this transformation was changed from EtOAc to toluene, the aminoarylation product 8 was formed *via* toluene C–H activation. A variety of substituted arenes can also be used in this transformation, with substituents including Br, CH<sub>3</sub>, and CH<sub>3</sub>O. Furthermore, mono-substituted arenes react with extremely high selectivity at the *para* position (*c.f.*, products 9–12 of Fig. 5). This high selectivity is in marked contrast to most other Pd-catalysed

functionalisations of mono-substituted arenes, which typically form mixtures of isomeric products.<sup>8</sup> Additionally, Michael's aminoarylations proceed efficiently at room temperature, which is significantly milder than most Pd<sup>II</sup>-catalysed C–H functionalisations of simple arenes. The authors propose that arene C–H activation occurs at a Pd<sup>IV</sup> centre and that this feature is responsible for the unusually high selectivity and reactivity.

A number of experiments were conducted to gain further insights into the mechanism of this process. First, the electronic requirements of the C–H activation step were investigated using competition experiments between benzene and other arenes. These studies showed that benzene reacts faster (by a factor of  $\sim 2.5$ ) than both anisole and bromobenzene.

A competition between toluene and toluene-*d*<sub>8</sub> showed an intermolecular H/D competition isotope effect of 1.1 (**14**-*d*<sub>0</sub>/**14**-*d*<sub>7</sub> = 1.1, Fig. 6a). In contrast, the use of 1,3,5-trideutero benzene as the substrate resulted in a much larger intramolecular H/D competition isotope effect of 4 (**15**-*d*<sub>3</sub>/**15**-*d*<sub>2</sub> = 4, Fig. 6b). In combination, these results implicate a 2-step C–H activation process, in which the two different steps occur with distinct selectivities. As shown in Fig. 7, the authors propose that the two steps are  $\pi$ -coordination of the arene to the Pd<sup>IV</sup> centre (which determines the intermolecular isotope effect, step (iii) in Fig. 7) followed by C–H cleavage of the  $\pi$ -coordinated substrate (which dictates the intramolecular isotope effect, step (iv) in Fig. 7). Notably, C–H activation reactions at Pd<sup>II</sup> centres generally show much higher intermolecular competition isotope effects (typically ranging from 2 to 6).<sup>9</sup>

On the basis of these (and additional) studies, a full catalytic cycle was proposed. As shown in Fig. 7, the cycle begins with intramolecular *anti*-aminopalladation to produce alkyl Pd<sup>II</sup> intermediate D (step (i)). D then undergoes oxidation with NFSI to produce Pd<sup>IV</sup> intermediate E (step (ii))  $\pi$ -coordination of the arene substrate to E to generate F (step (iii)) is followed by C–H cleavage (step (iv)) to afford aryl alkyl Pd<sup>IV</sup> complex G. Finally, C–C bond-forming reductive elimination (step (v)) closes the catalytic cycle.

The Yu group reported a related Pd<sup>II/IV</sup>-catalysed C–H functionalization reaction involving the oxidative coupling of per-fluorobenzamides with simple arenes using NFSI as the oxidant (Fig. 8).<sup>10</sup> Similar to Michael's work, this transformation proceeds with very high *para* selectivity, ranging from 12 : 1

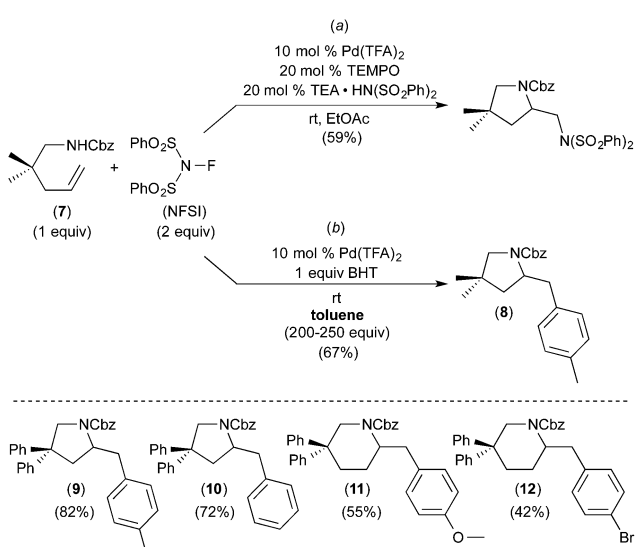


Fig. 5 Alkene aminoarylation via proposed C–H activation at Pd<sup>IV</sup>.

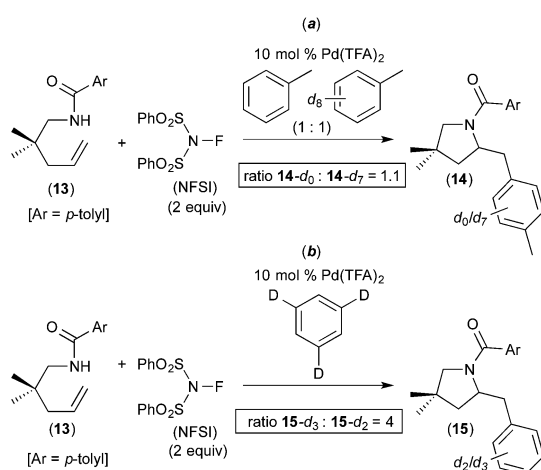


Fig. 6 Kinetic isotope effect studies of alkene aminoarylation reaction.

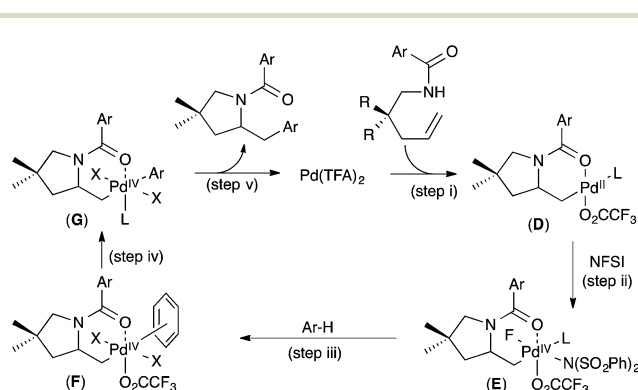


Fig. 7 Proposed mechanism for aminoarylation.



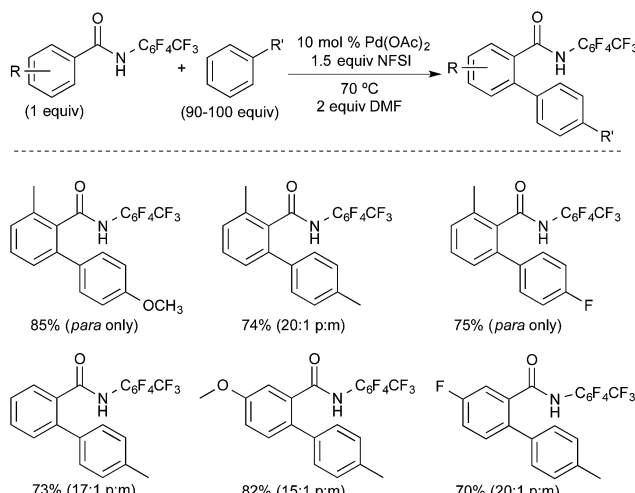


Fig. 8 Arene C–H oxidative coupling involving proposed C–H activation at  $\text{Pd}^{\text{IV}}$ .

with a bromo- or ethyl-substituent to “*para* only,” with methoxy- or fluoro-substituents. The authors rationalize this unusually high selectivity based on a mechanism involving two sequential C–H activation events: ligand-directed C–H activation at  $\text{Pd}^{\text{II}}$  followed by arene C–H activation at  $\text{Pd}^{\text{IV}}$ . They propose that the weakly coordinating perfluorobenzamide directs an initial C–H activation at  $\text{Pd}^{\text{II}}$ . The NFSI then oxidizes this palladacyclic intermediate to a  $\text{Pd}^{\text{IV}}$  fluoride complex, which promotes *para*-selective arene C–H activation.<sup>11</sup>

Several studies were conducted to shed further light on the mechanism of this transformation. While substantial yields of oxidative coupled products were obtained with a number of different oxidants (*e.g.*, Selectfluor, *N*-fluoropyridinium  $\text{K}_2\text{S}_2\text{O}_8$ ), only  $\text{F}^+$  oxidants afforded high levels of *para*-selectivity. This led the authors to propose that the presence of a fluoride ligand on the  $\text{Pd}^{\text{IV}}$  center is crucial for achieving *para*-selective C–H activation.

As shown in Fig. 9, an isotope effect study revealed that the initial reaction rate is identical with toluene and toluene- $d_8$  as the arene substrate ( $k_{\text{H}}/k_{\text{D}} = 1$ ). This result suggests that the C–H activation at  $\text{Pd}^{\text{IV}}$  is not the slow step of the catalytic cycle. Unlike the Michael system, no competition or intramolecular isotope effect studies were reported in this system, so the possible role of  $\pi$ -coordination cannot be assessed from this report.<sup>10</sup>

A number of groups have used naphthalene as a substrate in C–H arylation reactions that are believed to proceed *via* C–H activation at  $\text{Pd}^{\text{IV}}$ . For example, in 2008, Inoue and coworkers

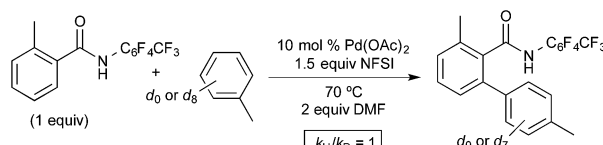


Fig. 9 Isotope effect study for arene C–H oxidative coupling.

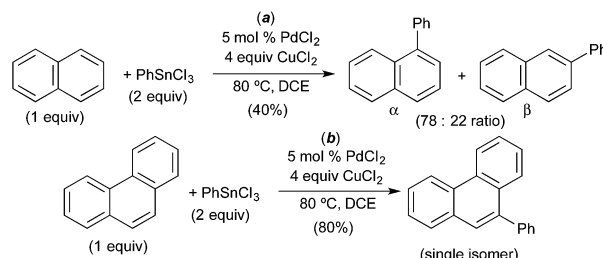


Fig. 10 C–H arylation of arenes with  $\text{PhSnCl}_3$  *via* proposed C–H activation at  $\text{Pd}^{\text{IV}}$ .

demonstrated the  $\text{PdCl}_2$ -catalysed C–H arylation of naphthalene with aryl stannanes.<sup>12</sup> This reaction was selective for arylation at the  $\alpha$ -position of naphthalene ( $\alpha : \beta$  ratio = 3.5 : 1, Fig. 10a) and afforded modest 40% yield. A variety of other substrates were evaluated and phenanthrene was found to afford the best yield (80%) as well as high selectivity for the 9-position (Fig. 10b). A mechanism involving naphthalene or phenanthrene C–H activation at  $\text{Pd}^{\text{IV}}$  was proposed; however, minimal evidence is provided to support this pathway.

More recently, our group demonstrated the C–H arylation of naphthalene using diaryliodonium salts as both the oxidant and aryl source (Fig. 11).<sup>13</sup> In this system, the selectivity of C–H cleavage could be tuned through the appropriate selection of supporting ligand. Simple Pd salts, such as  $\text{Pd}(\text{OAc})_2$  and  $\text{PdCl}_2$ , afforded modest yields and selectivities for the C–C coupled products (yields ranging from 12–24% and  $\alpha : \beta$  selectivities from 5 : 1 to 13 : 1). The yield and selectivity could be enhanced dramatically through the use of N–N chelating L type ligands, and the optimal diimine Pd catalyst (16 in Fig. 11) afforded 70% yield and  $>70 : 1$  selectivity for the  $\alpha$ -arylated product. Notably, since this work, complementary  $\beta$  selectivity has been achieved in the same transformation by employing a platinum catalyst.<sup>4c</sup>

Rate studies of the Pd-catalyzed naphthalene arylation showed 1<sup>st</sup> order kinetics in  $[\text{Ar}_2\text{I}]^+$  and zero order dependence on [naphthalene]. Isotope effect studies were conducted using naphthalene and naphthalene- $d_8$ . The initial rate of the C–H arylation reaction was essentially identical with each of these two substrates ( $k_{\text{H}}/k_{\text{D}} = 1$ , Fig. 12b). Furthermore, a competition between naphthalene and naphthalene- $d_8$  afforded a product ratio corresponding to an H/D competition isotope effect of 1.08 ( $17-d_0/17-d_7 = 1.08$ , Fig. 12a). This is very similar to the results obtained by Michael in analogous competition experiments (Fig. 6). Naphthalene was found to be the best substrate for this reaction, and arenes without an extended  $\pi$ -system (*e.g.*,

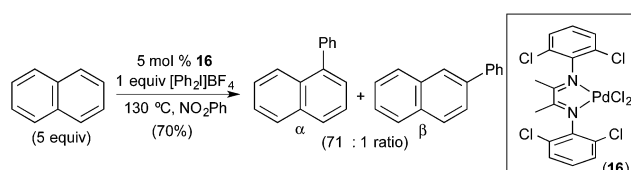


Fig. 11 C–H arylation of naphthalene with  $[\text{Ph}_2\text{I}]^{\text{BF}_4}$  *via* proposed C–H activation at  $\text{Pd}^{\text{IV}}$ .

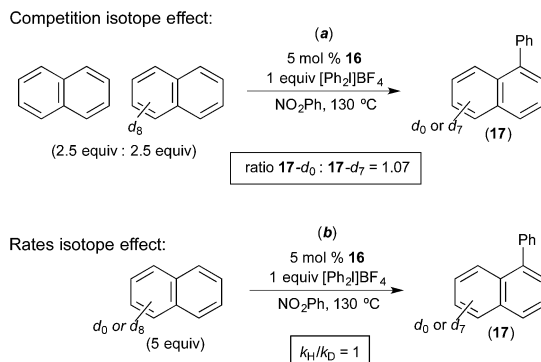
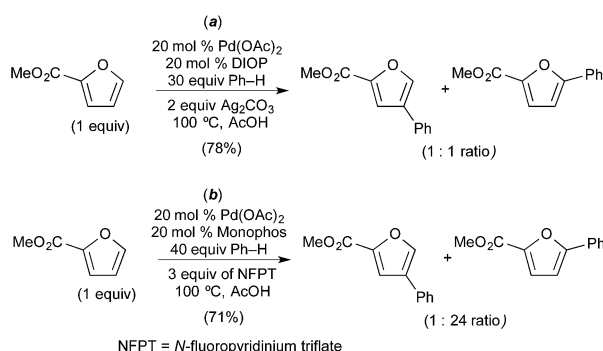
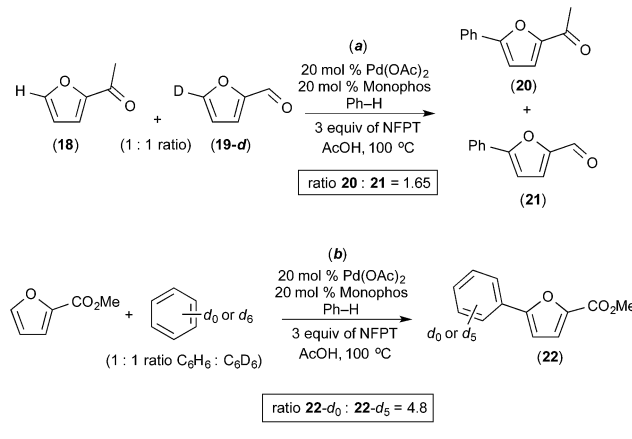


Fig. 12 Isotope effect studies of naphthalene C–H arylation.

anisole, benzene, chlorobenzene, veratrole) afforded low yields and selectivities. On the basis of these investigations, the oxidation of the  $\text{Pd}^{\text{II}}$  catalyst by the arylidonium salt was proposed to be the rate-determining step, and the C–H activation of naphthalene was proposed to occur at the resulting  $\text{Pd}^{\text{IV}}$  centre. Additionally, a two-step C–H activation mechanism analogous to that put forth by Michael (Fig. 7) was proposed in this system. The first step is proposed to involve  $\pi$ -coordination of the substrate to  $\text{Pd}^{\text{IV}}$  (a step that should be facilitated by the extended  $\pi$ -system of naphthalene) followed by subsequent C–H cleavage at the  $\text{Pd}^{\text{IV}}$  centre.

Seayad recently described the selective C–H/C–H oxidative coupling of furans with arenes (Fig. 13).<sup>14</sup> In this system, the site selectivity of furan C–H activation could be modulated based appropriate selection of the terminal oxidant. Using  $\text{Ag}_2\text{CO}_3$  as oxidant, the authors observed poorly selective activation of the furan (C-4/C-5 arylated products were formed in an  $\sim 1 : 1$  ratio, Fig. 13a). Notably,  $\text{Ag}_2\text{CO}_3$  is unlikely to promote oxidation of  $\text{Pd}^{\text{II}}$  to  $\text{Pd}^{\text{IV}}$ . In contrast, the use of *N*-fluoropyridinium triflate (NFTP), an “F<sup>+</sup>” oxidant that is well known to promote the oxidation of  $\text{Pd}^{\text{II}}$  to  $\text{Pd}^{\text{IV}}$ ,<sup>15</sup> afforded  $>20 : 1$  C-5 selectivity in most cases. In the NFTP system, large isotope effect (ratio of products  $22\text{-}d_0/22\text{-}d_5 = 4.8$ ) was observed when the reaction was run as a competition between benzene and benzene- $d_6$  (Fig. 14b). In contrast, the competition between furan **18** and deuterated furan **19-d** resulted in a relatively small quasi isotope

Fig. 13 Oxidative coupling of furans and benzene: proposed furan C–H activation at  $\text{Pd}^{\text{II}}$  (a) and  $\text{Pd}^{\text{IV}}$  (b) depending on oxidant.

NFPT = *N*-fluoropyridinium triflate

Fig. 14 Isotope effect studies in benzene/furan oxidative coupling with NFPT as oxidant.

effect of 1.7 (the substrates are slightly different, so this is not a true isotope effect; however, the authors state that the rate of arylation is similar for the two substrates) (Fig. 14a). The authors propose a mechanism initiated by initial oxidation of ligated  $\text{Pd}^{\text{II}}$  to  $\text{Pd}^{\text{IV}}$  by NFPT and subsequent C–H activation of the two substrates. An alternative possibility involving benzene activation at  $\text{Pd}^{\text{II}}$ , oxidation with NFPT and subsequent furan activation at  $\text{Pd}^{\text{IV}}$  is also possible, and perhaps more likely based on the related reactions described above.

The examples described above summarize the current state of the art in catalytic transformations proposed to proceed *via* C–H activation at  $\text{Pd}^{\text{IV}}$ . These examples show encouraging selectivity trends and demonstrate that valuable synthetic methods can be achieved with C–H activation at  $\text{Pd}^{\text{IV}}$  as a likely step. At this stage, most of these transformations have been discovered serendipitously rather than through reaction design. However, moving forward it would be important to rationally design catalytic sequences involving C–H activation at a  $\text{Pd}^{\text{IV}}$  centre. A uniting feature of the transformations discussed above is the use of strong oxidants, with “F<sup>+</sup>” reagents, hypervalent iodine reagents, and inorganic peroxides being particularly common choices. In addition, many of these transformations are believed to involve the generation of a  $\text{Pd}^{\text{II}}\text{–C}$  bond prior to oxidation of  $\text{Pd}^{\text{II}}$  to  $\text{Pd}^{\text{IV}}$ . This likely serves to accelerate the oxidation event. Finally, most of the catalysts and intermediates in these transformations possess oxidatively stable ligands that are unlikely to participate in competing reductive elimination. All of these features should serve as key design considerations as new reactions are developed.

## Direct observation of C–H activation at $\text{Pd}^{\text{IV}}$

Our group has developed organometallic model systems in order to directly observe and study this fundamental reaction. Such studies should ultimately assist in the rational design of new catalytic processes that incorporate this elementary step.



The  $\text{Pd}^{\text{IV}}$  model complexes were carefully designed to accelerate C–H activation while slowing competing reductive elimination processes from  $\text{Pd}^{\text{IV}}$ . These complexes were designed so that the C–H activation would be intramolecular. For example, in complex **24** (Fig. 15), studied by Racowski *et al.*,<sup>16</sup> the biphenyl ligand was incorporated to enable intramolecular C–H activation, which is typically more facile than the corresponding intermolecular reactions. In addition, the  $\text{CF}_3$  ligand was included because aryl- $\text{CF}_3$  reductive elimination is known to be relatively slow from  $\text{Pd}^{\text{IV}}$ , particularly at low temperatures.<sup>17</sup> Complex **24** was generated *in situ* by the oxidation of (bpy)Pd<sup>II</sup>(2-biphenyl) ( $\text{CF}_3$ ) complex **23** with  $\text{PhICl}_2$  at  $-30\text{ }^{\circ}\text{C}$ . Warming complex **24** to room temperature resulted in intramolecular activation of the 2-aryl substituent to form the cyclometalated  $\text{Pd}^{\text{IV}}$  product **25**. To our knowledge, this was the first direct observation of C–H activation at a  $\text{Pd}^{\text{IV}}$  centre.

In a follow up study, the related complex **26** (Fig. 16) was synthesized *via* oxidation of a  $\text{Pd}^{\text{II}}$  precursor with  $\text{PhICl}_2$ .<sup>18</sup> The tridentate tris(2-pyridyl)-methane ligand ( $\text{Py}_3\text{CH}$ ) was a key design feature in this study. This strongly coordinating tridentate ligand is well-known to stabilize octahedral  $\text{Pd}^{\text{IV}}$  species relative to analogues with bidentate nitrogen donors like bipyridine.<sup>19</sup> Thus, it was anticipated that the  $\text{Py}_3\text{CH}$  ligand would slow C–H activation and enable more detailed mechanistic investigations of this process. Indeed, the  $\text{Pd}^{\text{IV}}$  aryl complex **26** proved stable at room temperature and could be fully characterized by 1D and 2D NMR, HRMS, and X-ray crystallography. Complex **26** did not undergo C–H activation, even upon heating to  $90\text{ }^{\circ}\text{C}$  in  $\text{CDCl}_3$ . Instead, C–Cl bond-forming reductive elimination was observed under these conditions. However, when one of the chloride ligands in **26** was exchanged for an acetate, the resulting intermediate **27** underwent clean cyclometalation at room temperature to yield **28**. This result suggests that C–H activation at  $\text{Pd}^{\text{IV}}$  in this system likely occurs *via* a concerted metalation-deprotonation mechanism, analogous to C–H activation at  $\text{Pd}^{\text{II}}$ .<sup>20</sup>

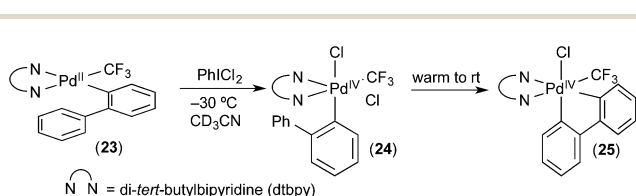


Fig. 15 First direct observation of C–H activation at  $\text{Pd}^{\text{IV}}$ .

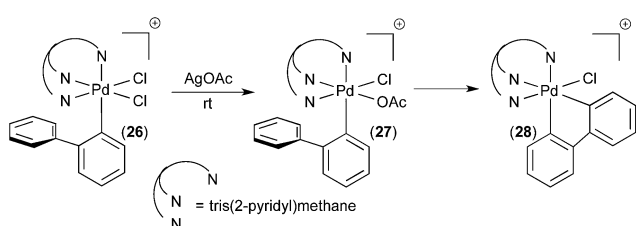


Fig. 16 C–H activation at  $\text{Pd}^{\text{IV}}$  complex **27**.

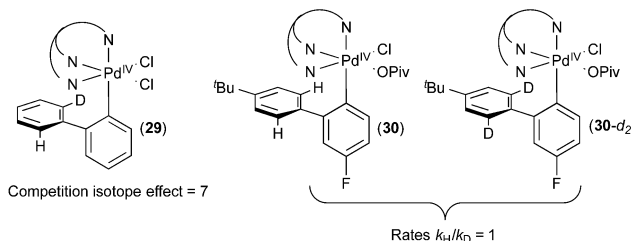


Fig. 17 Isotope effects in C–H activation at  $\text{Pd}^{\text{IV}}$ .

When complex **29** (Fig. 17) was treated with acetate, a product ratio consistent with an H/D competition isotope effect of 7 was obtained. In contrast, the initial rate of C–H activation at **30** *versus* **30-*d*<sub>2</sub>** was essentially identical ( $k_{\text{H}}/k_{\text{D}} = 1$ ). These results in combination with a variety of studies of the dynamic behaviour of complex **26** indicate that C–H cleavage is not the rate determining step in the C–H activation process in this system. The similarity between the KIE observed on this system to those observed in catalytic systems further supports the mechanisms proposed for the catalytic reactions described above.

These two examples chronicle C–H activation at discrete and, in one case, isolable  $\text{Pd}^{\text{IV}}$  complexes. It is also noteworthy that C–H activation at the  $\text{Pd}^{\text{IV}}$  centre can be facile at room temperature or below with bidentate ligands or in the presence of acetate ion. Future work on isolated palladium complexes may explore an intermolecular C–H activation event at  $\text{Pd}^{\text{IV}}$ .

## Conclusions

The catalytic functionalization of C–H bonds *via* high valent palladium is a powerful manifold for developing synthetically useful transformations. This mini-review has summarized experiments supporting the viability of C–H bond activation at  $\text{Pd}^{\text{IV}}$  and has described mechanistic studies of the C–H bond cleavage event. Synthetically useful catalytic cycles that utilize C–H activation at  $\text{Pd}^{\text{IV}}$  remain limited; however, there are great opportunities in this area due to the potential for unique selectivity in these transformations. Although the presently described work is mostly limited to catalytic C–H arylation sequences, as this method is more fully understood, one can anticipate its application to more diverse scaffolds and functionalizations.

## Acknowledgements

We thank the NIH (GM073836) and NSF (CHE-1111563 and CHE-1361542) for support of this research. In addition, JJT gratefully acknowledges the NIH (F32 GM109479) for a post-doctoral fellowship.

## Notes and references

- For reviews on C–H activation: (a) A. D. Ryabov, *Chem. Rev.*, 1990, **90**, 403; (b) A. E. Shilov and G. B. Shul'pin, *Chem. Rev.*, 1997, **97**, 2879; (c) V. Ritleng, C. Sirlin and M. Pfeffer, *Chem.*



*Rev.*, 2002, **102**, 1731; (d) A. R. Dick and M. S. Sanford, *Tetrahedron*, 2006, **62**, 2439; (e) I. A. I. Mkhald, J. H. Barnard, T. B. Marder, J. M. Murphy and J. F. Hartwig, *Chem. Rev.*, 2010, **110**, 890; (f) M. P. Doyle, R. Duffy, M. Ratnikov and L. Zhou, *Chem. Rev.*, 2010, **110**, 704; (g) H. M. Davies, J. Du Bois and J. Q. Yu, *Chem. Soc. Rev.*, 2011, **40**, 1855; (h) D. A. Colby, R. G. Bergman and J. A. Ellman, *Chem. Rev.*, 2009, **110**, 624.

2 For reviews on C–H activation at Pd<sup>II</sup>: (a) X. Chen, K. M. Engle, D. Wang and J. Q. Yu, *Angew. Chem., Int. Ed.*, 2009, **48**, 5094; (b) T. W. Lyons and M. S. Sanford, *Chem. Rev.*, 2010, **110**, 1147; (c) L. Ackermann, *Chem. Rev.*, 2011, **111**, 1315; (d) S. R. Neufeldt and M. S. Sanford, *Acc. Chem. Res.*, 2012, **45**, 936.

3 (a) D. C. Powers, E. Lee, A. Ariaford, M. S. Sanford, B. F. Yates, A. J. Carty and T. Ritter, *J. Am. Chem. Soc.*, 2012, **134**, 12002; (b) D. C. Powers and T. Ritter, *Acc. Chem. Res.*, 2012, **45**, 840.

4 For reports proposing allylic and/or vinylic C–H activation at Pd<sup>IV</sup>: (a) L. T. Pilarski, N. Selander, D. Bose and K. J. Szabo, *Org. Lett.*, 2009, **11**, 5518; (b) N. Selander, B. Willy and K. J. Szabo, *Angew. Chem., Int. Ed.*, 2010, **49**, 4051; (c) R. Alam, L. T. Pilarski, E. Pershagen and K. J. Szabo, *J. Am. Chem. Soc.*, 2012, **134**, 8778.

5 For examples of C–H activation at Pt<sup>IV</sup> see: (a) G. B. Shul'pin, G. V. Nizova and A. T. Nikitaev, *J. Organomet. Chem.*, 1984, **276**, 115; (b) M. Lersch and M. Tilset, *Chem. Rev.*, 2005, **105**, 2471; (c) A. M. Wagner, A. J. Hickman and M. S. Sanford, *J. Am. Chem. Soc.*, 2013, **135**, 15110.

6 K. L. Hull, E. L. Lanni and M. S. Sanford, *J. Am. Chem. Soc.*, 2006, **128**, 14047.

7 (a) C. F. Rosewall, P. A. Sibbald, D. V. Liskin and F. E. Michael, *J. Am. Chem. Soc.*, 2009, **131**, 9488; (b) P. A. Sibbald, C. F. Rosewall, R. D. Swartz and F. E. Michael, *J. Am. Chem. Soc.*, 2009, **131**, 15945.

8 For examples of modest selectivity for C–H activation at Pd<sup>II</sup>, see ref. 1b and 2d as well as: (a) Y. Fujiwara, R. Asano, I. Moritani and S. Teranishi, *J. Org. Chem.*, 1976, **41**, 1681; (b) L. J. Ackerman, J. P. Sadighi, D. M. Kurtz, J. A. Labinger and J. E. Bercaw, *Organometallics*, 2003, **22**, 3884.

9 Examples of isotope effects for C–H activation at Pd<sup>II</sup>: (a) H. A. Chiong, Q. Pham and O. J. Daugulis, *J. Am. Chem. Soc.*, 2007, **129**, 9879; (b) Z. J. Shi, B. Li, X. Wan, J. Cheng, Z. Fang, B. Cao, C. Qin and Y. Wang, *Angew. Chem., Int. Ed.*, 2007, **46**, 5554; (c) M. Lafrance and K. Fagnou, *J. Am. Chem. Soc.*, 2006, **128**, 16496.

10 X. Wang, D. Leow and J. Q. Yu, *J. Am. Chem. Soc.*, 2011, **133**, 13864.

11 (a) K. Engle, T. S. Mei, X. Wang and J. Q. Yu, *Angew. Chem., Int. Ed.*, 2011, **50**, 1478; (b) A. J. Hickman and M. S. Sanford, *Nature*, 2012, **484**, 177.

12 H. Kawai, Y. Kobayashi, S. Oi and Y. Inoue, *Chem. Commun.*, 2008, 1464.

13 A. J. Hickman and M. S. Sanford, *ACS Catal.*, 2011, **1**, 170.

14 N. Asyikin, B. Juwaini, J. K. P. Ng and J. Seayad, *ACS Catal.*, 2012, **2**, 1787.

15 (a) N. D. Ball and M. S. Sanford, *J. Am. Chem. Soc.*, 2009, **131**, 3796; (b) N. B. Ball, J. W. Kampf and M. S. Sanford, *J. Am. Chem. Soc.*, 2010, **132**, 2878; (c) J. M. Racowski, J. B. Gary and M. S. Sanford, *Angew. Chem., Int. Ed.*, 2012, **51**, 3414.

16 J. M. Racowski, N. D. Ball and M. S. Sanford, *J. Am. Chem. Soc.*, 2011, **133**, 18022.

17 N. D. Ball, J. B. Gary, Y. Ye, J. Kampf and M. S. Sanford, *J. Am. Chem. Soc.*, 2011, **133**, 7577.

18 A. Maleckis, J. W. Kampf and M. S. Sanford, *J. Am. Chem. Soc.*, 2013, **135**, 6618.

19 (a) P. K. Byers, A. J. Carty, B. W. Skelton and A. H. White, *J. Chem. Soc., Chem. Commun.*, 1987, 1093; (b) P. K. Byers, A. J. Carty, B. W. Skelton and A. H. White, *Organometallics*, 1990, **9**, 826.

20 (a) D. L. Davies, S. M. A. Donald and S. A. Macgregor, *J. Am. Chem. Soc.*, 2005, **127**, 13754; (b) M. Lafrance and K. Fagnou, *J. Am. Chem. Soc.*, 2006, **128**, 16496; (c) S. I. Gorelsky, D. Lapointe and K. Fagnou, *J. Am. Chem. Soc.*, 2008, **130**, 10848.

